



Multibudded tubules formed by COPII on artificial liposomes

SUBJECT AREAS:

MEMBRANE
TRAFFICKING

BIOPHYSICAL CHEMISTRY

IMAGING
CELL BIOLOGY

Kirsten Bacia^{1,3}, Eugene Futai^{1*}, Simone Prinz², Annette Meister³, Sebastian Daum³, Daniela Glatte³, John A. G. Briggs² & Randy Schekman¹

¹Dept. of Molecular and Cell Biology, University of California, Berkeley, CA 94720-3202, USA, ²Structural and Computational Biology Unit, European Molecular Biology Laboratory, Meyerhofstrasse 1, 69117 Heidelberg, Germany, ³HALOmem, University of Halle, Kurt-Mothes-Str. 3, 06120 Halle, Germany.

Received
08 February 2011

Accepted
23 May 2011

Published
17 June 2011

COPII-coated vesicles form at the endoplasmic reticulum for cargo transport to the Golgi apparatus. We used *in vitro* reconstitution to examine the roles of the COPII scaffold in remodeling the shape of a lipid bilayer. Giant Unilamellar Vesicles were examined using fast confocal fluorescence and cryo-electron microscopy in order to avoid separation steps and minimize mechanical manipulation. COPII showed a preference for high curvature structures, but also sufficient flexibility for binding to low curvatures. The COPII proteins induced beads-on-a-string-like constricted tubules, similar to those previously observed in cells. We speculate about a mechanical pathway for vesicle fission from these multibudded COPII-coated tubules, considering the possibility that withdrawal of the Sar1 amphipathic helix upon GTP hydrolysis leads to lipid bilayer destabilization resulting in fission.

Correspondence and requests for materials should be addressed to R.S. (schekman@berkeley.edu)

* Current address: Dept. of Agriculture, Tohoku University, Sendai, Miyagi 981-8555, Japan

Because of their compartmentalized structure, eukaryotic cells require pathways for trafficking cargo between lipid-bilayer-enclosed organelles. The most prominent pathways involve coat proteins that help recruit cargo and shape the lipid bilayer into small, highly curved vesicles. Assembly of the COPII coat, involved in ER-to-Golgi traffic, requires the Arf-like GTPase Sar1. When activated by Sec12, the guanine-nucleotide exchange factor, Sar1 exposes an N-terminal amphipathic helix (AH), which embeds in the membrane, and recruits the Sec23/Sec24 and Sec13/Sec31 complexes. In addition to coat recruitment, it was shown that Sar1 has a role in vesicle fission^{1,2}. The mechanical pathway of COPII vesicle formation and separation from ER membranes, however, has been difficult to pin down.

In a biochemical *in vitro* 'budding assay' using liposomes and density gradient centrifugation (or conventional EM for visualization) vesicles are most efficiently produced with COPII and non-hydrolysable GTP, suggesting that the activated conformation of Sar1 is sufficient for budding. However, Sar1 mutants restricted to GTP in the non-hydrolysed state block cargo transport *in vivo* (yeast Sar1p(H77L)³ and mammalian Sar1(H79G)⁴). Among possible explanations for this discrepancy is a 'trituration' artifact caused by centrifugation steps during *in vitro* sample preparations⁵.

To investigate this possibility and avoid centrifugation, we replaced the 400 nm liposomes by Giant Unilamellar Vesicles (GUVs), which allows direct visualization by confocal microscopy. No manipulation was required after initial mixing of COPII proteins and GUVs. In addition, electron microscopy (EM) was performed using negative stain and cryo-EM. GUVs were found to be suitable for cryo-EM preparations and superior to Large Unilamellar Vesicles (LUVs), because of larger membrane reservoirs and higher unilamellarity.

Our results suggest that tubular structures at ER exit sites observed both *in vitro* and *in vivo* constitute a functional basis for COPII vesicle formation, possibly permitting the transport of large cargo. Our results offer a possible explanation for the difference in Sar1-GTP behavior previously observed *in vitro* and *in vivo*.

Results

Sar1p-GTP is a strong inducer of membrane curvature. Activated Sar1p induces highly curved membrane tubules with narrow diameters, down to ≈ 26 nm^{2,6}. For a dynamic *in situ* view, we observed the tubulation of lipid-labeled GUVs, using fast line-scanning microscopy (Fig. 1). Incubations contained Sar1p, Sec12 Δ Cp¹ and a GTP-regenerating system (GTP_r) to maximize Sar1p loading with GTP. To avoid osmotic effects, osmolarities were adjusted. Rapid tubulation increased membrane tension, resulting in GUV rupture and collapse into dense balls of soft tubules (Fig. 1b–d, Movie S1). Because GTP hydrolysis by Sar1 is slow in the absence of GTPase activating proteins of the outer coat, wtSar1p with hydrolysable GTP (Fig. 1b–e), the mutant Sar1p(H77L) with

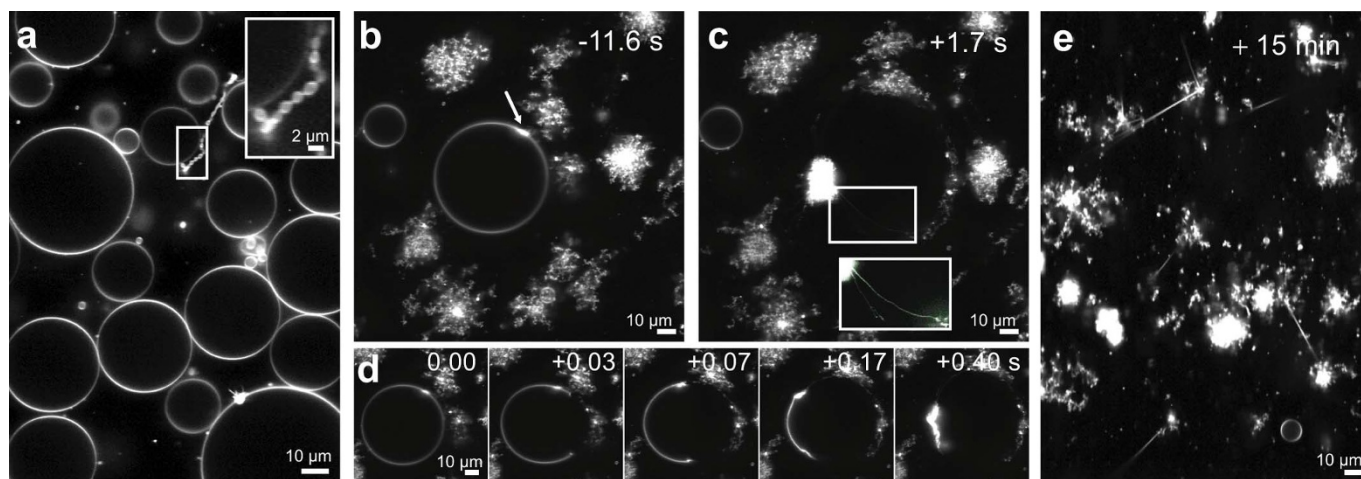


Figure 1 | Membrane tubulation by Sar1p. Confocal microscopy of fluorescently labeled membranes. (a) Sar1p-GDP control: GUVs remained mostly unaffected. A minority of μm -sized pearly vesicles was observed (inset) [$2\mu\text{M}$ Sar1p, $1\mu\text{M}$ Sec12 ΔCp , 1mM GDP]. (b–d) GUV tubulation by Sar1p-GTP [$1\mu\text{M}$ Sar1p, $0.5\mu\text{M}$ Sec12 ΔCp , 1mM GTP $_{\gamma}$]. (b) Tubulation starts (arrow). (c) The GUV has exploded into a ‘ball’ of thin, wiggling membrane tubules. The inset shows tubules at increased contrast. (d) Timeseries of the explosion. See also Movie S1. (e) Straight, rigid lipid tubules after prolonged incubation with Sar1p-GTP.

GTP (Fig. S1d) and wtSar1p with non-hydrolysable GMP-PNP all resulted in liposome tubulation. In incubations of wtSar1p and Sar1p(H77L) with GTP, prominent straight and rigid tubules appeared (Fig. 1e and Fig. S1d,⁶). These exhibited brighter fluorescence and sometimes fraying ends, suggesting bundles. Control incubations without active Sar1p (Fig. 1a, S1a–c) yielded mostly intact GUVs with a low level of tubules and pearly vesicles⁷.

COPII forms rigid tubules. When giant liposomes were incubated with the full COPII coat (Sar1p, Sec23/24p and Sec13/31p) in the presence of GTP, confocal microscopy showed a heterogeneous picture, consisting of intact GUVs, ‘granulated’ GUVs, tubules, small and larger vesicles and aggregated membranes (Fig. 2h,i). A biochemical budding assay that involved sucrose gradient centrifugation did not show a distinguishable budded vesicle fraction in incubations containing GTP¹⁸. A clear fraction of budded vesicle was only observed with non-hydrolysable GMP-PNP, suggesting that the minimal COPII system used *in vitro* lacks factors that govern the spatial and temporal coordination of fission. We therefore adopted the GMP-PNP condition that produces robust vesicle formation in the biochemical assay for use in our GUV assay.

The generally accepted picture of budding depicts vesicles as forming from single-vesicle-buds^{9,10}. Taken together with the positive budding results by Matsuoka et al.⁸, we expected to obtain separated COPII vesicles in incubations of GUVs with COPII proteins and GMP-PNP. Because COPII vesicles are below optical resolution, we expected a hazy fluorescence background in the space outside the mother liposomes. This was not observed. Instead, prominent straight and rigid extensions were formed (Fig. 2b, Movie S2). Some GUVs appeared fully tubulated. Others were densely covered with COPII-coated extensions that remained connected to the GUV, yielding a ‘star-fish’ like appearance. Some extensions were more than $10\mu\text{m}$ long. Notably, the persistence length was much greater than the length of the tubules. Fluorescence intensity was fairly uniform, indicating that all tubular extensions had a uniform, defined thickness.

COPII shows a preference for high curvature structures. The COPII protein coat was clearly localized on the rigid extensions, as seen from a comparison of the fluorescence signals of the lipid and the Sec13/31 coat (Fig. 2c). In fact, more COPII was bound to the highly curved extensions than to the low curvature GUV surface.

This implies that the COPII complex plays a role in remodeling the lipid bilayers into highly curved structures or that it preferentially binds highly curved surfaces, presumably stabilizing them.

The COPII proteins act jointly in membrane deformation. No differences in rigid tubulation were observed if nucleotide exchange on Sar1p was achieved by the addition of EDTA to lower Mg^{2+} (e.g., Fig. 2b) or by the addition of Sec12 ΔCp (e.g., Fig. 2c). The presence of the N-terminal amphipathic helix of Sar1p was required for COPII recruitment (Fig. 2g). At a reduced concentration (one-tenth) of Sar1p, tubules nonetheless formed, albeit with a lower yield (Fig. 2f). We also noted that the outer Sec13/31p coat complex was required to observe separated tubules. When Sec13/31p was omitted as in reconstitution experiments of pre-budding complexes¹¹, the GUVs aggregated, suggesting exposed hydrophobic contacts on the incomplete COPII coat (Fig. 2e vs. 2d, Fig. S2). These observations confirm the importance of Sar1p and the coordinated action of the COPII proteins.

Electron microscopy reveals multibudded tubules. Because the diameter of COPII-coated tubules is below the optical resolution of confocal microscopy, we used EM for a more detailed examination. Cryo-EM revealed that the COPII-coated tubules carry symmetric constrictions at regular intervals (Fig. 3). In other words, they consist of unfissioned vesicles, like beads on a string. The size of the connected vesicles in cryo-EM was rather homogeneous (Fig. 3a–h), although variations occurred, for instance at the end of a string (Fig. 3e). Apart from the prominent connected protein-coated vesicles, single vesicles as well as larger liposomes were observed (Fig. 3a,d–h).

Most beads-on-a-string vesicles were linearly connected, with occasional branches. Clover shapes, which appeared as branches, actually comprised two crossed-over tubules (Fig. 3a,b,f). Some of the constricted tubules deposited on the carbon support of the EM grid were up to several micrometers long and completely straight (Fig. 3f), whereas others apparently became entangled during the preparation (Fig. 3a). Except for the constrictions, tubules were mostly uniform in thickness. The appearance of the tubules in cryo-EM hence agreed well with their appearance by confocal microscopy. Furthermore, the cryo-EM images clearly showed protein coat on the lipid bilayer (Fig. 3b,d,e, arrows), even at the ‘necks’ between bulges, explaining the great persistence length. Whereas the typical

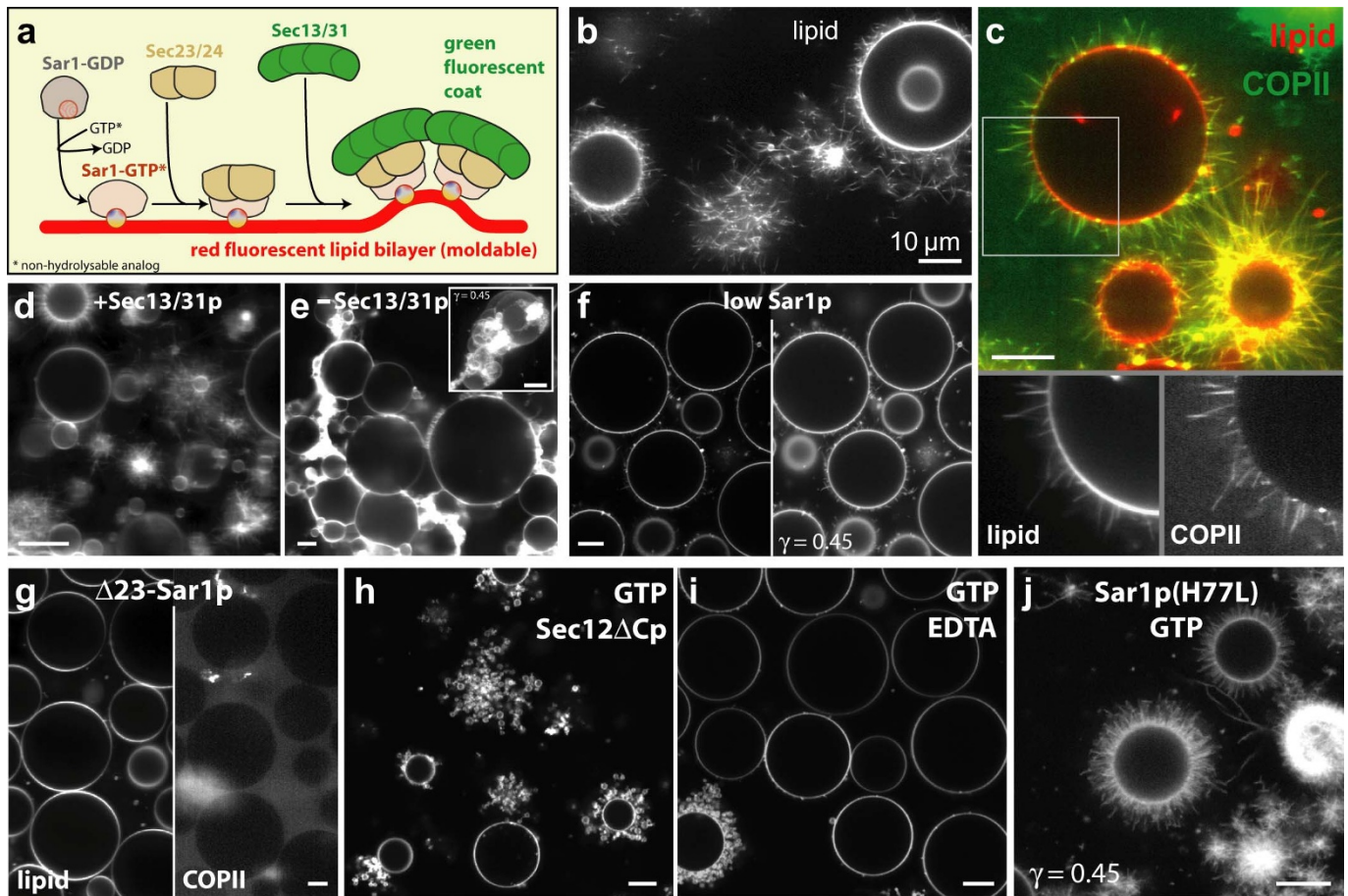


Figure 2 | Generation of rigid membrane extensions by COPII, visualized by confocal microscopy. Scale bars = 10 μm . (a) Schematic view. The reaction was reconstituted *in vitro* by mixing purified red fluorescent GUVs and purified COPII components [2 μM Sar1p, 320nM Sec23/24p, 520nM Sec13/31p; 1 μM Sec12 ΔCp or 2.5mM EDTA (to facilitate nucleotide exchange)]. (b) COPII produced long, rigid membrane extensions that appeared tubular at confocal microscopy resolution. (c) Green fluorescently labeled Sec13/31p showed a preferential COPII localization at highly curved tubules compared to the low curvature GUV. (d/e) Sec13/31p was essential. Extensive rigid tubulation was observed with full COPII and GMP-PNP (even at lowered COPII concentrations: 1 μM Sar1p, 160nM Sec23/24p, 260nM Sec13/31p, 2.5mM EDTA, 0.1mM GMP-PNP in panel d). In contrast, in the absence of Sec13/31p, GUVs and smaller liposome material aggregated (panel e). Inset: 3D maximum intensity projection (nonlinear intensity scale). Omitting Sec13/31p from the coat caused GUVs to adhere to each other. See also Fig. S2. (f) At concentrations of only 0.2 μM Sar1p [320nM Sec23/24p, 520nM Sec13/31p, 1 μM Sec12 ΔCp , 1mM GMP-PNP] mostly intact GUVs were observed. Close inspection revealed shorter rigid tubules emanating from the GUVs. Extensions are more easily discernible when using a nonlinear intensity scale (right). (g) The N-terminal amphipathic helix of Sar1p was essential for recruiting COPII. The truncated Δ23 mutant did not recruit COPII marked by a green labeled Sec13/31p (right) to the red labeled lipid bilayer (left) and did not induce tubulation of GUVs [2 μM Δ23 -Sar1p, 320nM Sec23/24p, 520nM Sec13/31p, 1 μM Sec12 ΔCp , 1mM GMP-PNP]. (h) With hydrolysable GTP, the COPII proteins produced a different and more heterogeneous picture consisting of intact GUVs, micron-sized vesicles and soft tubules [2 μM Sar1p, 320nM Sec23/24p, 520nM Sec13/31p, 1 μM Sec12 ΔCp , 1mM GTP]. (i) With EDTA instead of Sec12 ΔCp , GUVs appeared mostly intact, but some had a granular appearance or were surrounded by micron-sized vesicles [2 μM Sar1p, 320nM Sec23/24p, 520nM Sec13/31p, 2.5mM EDTA, 1mM GTP]. (j) In contrast to panels (h) and (i), the Sar1p mutant H77L as part of the COPII coat generated long, straight, rigid extensions with hydrolysable GTP [2 μM Sar1p(H77L), 320nM Sec23/24p, 520nM Sec13/31p, 1 μM Sec12 ΔCp , 1mM GTP].

strings of vesicles were all coated with protein, some of the larger liposomes appeared coated (Fig. 3d,e arrows) and others not (Fig. 3e, arrowhead). This observation seems to suggest that - despite the preference of the COPII coat for high-curvature structures seen by fluorescence - COPII proteins have some flexibility for binding to lower curvature membranes. The ability of the COPII coat to bind to membranes of different curvatures merits further investigation to determine how COPII cages form on 'oversized' cargo such as procollagen and chylomicrons^{12,13}.

Discussion

In vitro reconstitution experiments with artificial lipid bilayers, COPII proteins and non-hydrolysable GTP analog can be performed in different ways, involving different degrees of mechanical processing and separation: (i) Reactions of GUVs with COPII and

GMP-PNP without any centrifugation step yielded very long vesicle strings, shorter strings and some single vesicles (this work, Fig. 3a-h). (ii) Reactions of LUVs with COPII and GMP-PNP visualized by EM after chemical fixation and sedimentation showed buds, single vesicles and short strings of vesicles². (iii) Reactions of LUVs with COPII and GMP-PNP that were ultracentrifuged on a gradient contained a homogeneous fraction of small coated vesicles⁸. Together, these observations suggest that the vesicle strings formed with non-hydrolysable GTP analog may be precursors to single vesicles. Moreover, *in vitro* scission appears to be promoted by mechanical force.

It was previously noted that COPII vesicles produced *in vitro* have a similar appearance and diameter as native ones⁸. By keeping sample manipulation minimal, we have now been able to observe extended constricted tubules *in vitro* (Fig. 3a-h) and found that they exhibit strikingly similar shapes and diameters to those seen in

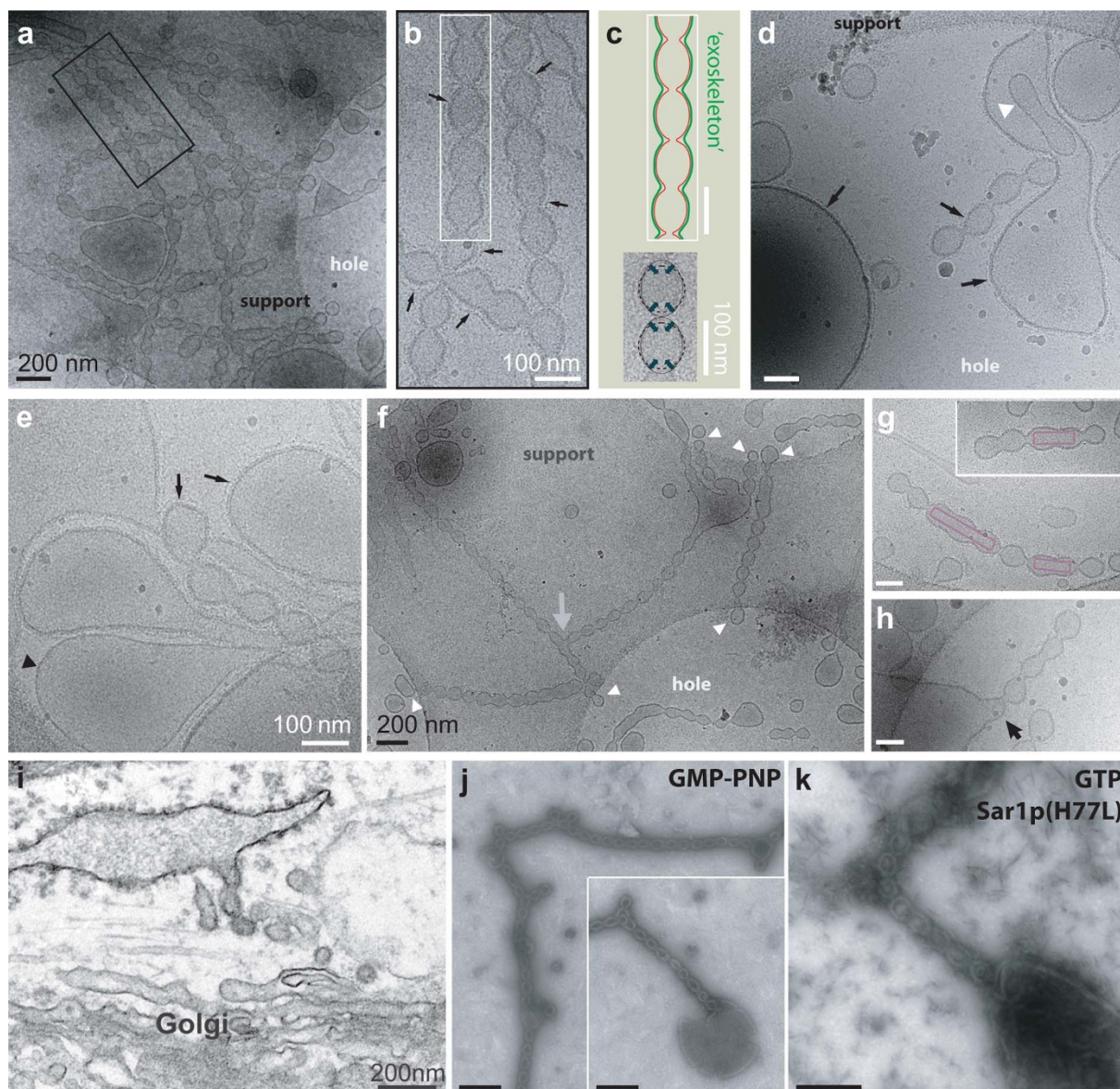


Figure 3 | Generation of multibudded structures by COPII, revealed by EM. Black scale bars = 200 nm; white = 100 nm. (a–h) Cryo-EM view of membrane extensions generated by COPII [2 μ M Sar1p, 320nM Sec23/24p, 520nM Sec13/31p, 2.5mM EDTA, 1mM GMP-PNP]. (a) Overview and (b) magnified inset. Tubular extensions were coated (arrows in panel b) and carried constrictions at \approx 100 nanometer spacing. (c) Schematic view and model: Drawing of a COPII vesicle string based on cryo-EM. Red denotes the lipid bilayer, green the protein coat. The COPII coat is rigid and may act like an exoskeleton. Bottom: Multibudded vesicles showed elongated shapes. A propensity of the COPII coat to form spheres may contribute to fission at the necks. (d,e) Both large and small vesicles were coated (d,e: arrows), but some large vesicles remained uncoated (e: black arrowhead). An internal vesicle (d: white arrowhead) remained uncoated. (f) Network of multibudded tubules. Occasional branches are seen in (a) and (f) [gray arrow]. Clover-shapes constituted cross-over tubules. Vesicle strings were apparently well-preserved on the carbon support, but often ended at the holes through which the solution had been blotted (white arrowheads). (g) Reconstituted vesicle strings suggest a mechanism for transport of large cargo. Hypothetical cargo is depicted as boxes. A 300 nm long procollagen bundle, for instance, may occupy three consecutive buds, with fission occurring at the adjoining necks. (h) Some vesicle strings were still connected to a larger liposome and appeared similar to ER exit sites in cells. (i) EM of ER exit sites in a wild type fibroblast cell showed multibudded tubules with a striking resemblance to those produced *in vitro* from artificial liposomes. (j) Multibudded tubules (including occasional branches) in reconstituted samples were also revealed by negative stain EM. The inset shows a multibudded tubule emanating from a collapsed liposome [2 μ M Sar1p, 320nM Sec23/24p, 520nM Sec13/31p, 2.5mM EDTA, 1mM GMP-PNP]. (k) The use of the GTP-locked Sar1p(H77L) mutant produced multi-budded tubules in the presence of hydrolysable GTP (negative stain; same sample as in Fig. 2j).

cells (Fig. 3i, ref. ^{14–16}). In cells, single vesicles, “dumb-bell shapes”, “tubular membranes with vesicular-shaped endings”¹⁶ and short “beaded necklaces”¹⁵ have been observed. Networks of longer vesicle strings with occasional branches were reported when GTP hydrolysis was blocked by the Sar1(H79G) mutation. This led to the suggestion that “budding continues in the absence of GTP hydrolysis, but [...] vesicles fail to complete separation from one another.”¹⁵

Our *in vitro* reconstitution results strongly parallel these *in vivo* observations. With nonhydrolysable GMP-PNP, extended necklace-like vesicle strings with various degrees of constrictions and occasional branches were observed (Fig. 3a–h). Vesicle pairs resembled dumb-bells. Nearly tubular sections were connected to vesicular-shaped endings. This diverse set of lipid structures that carry some level of COPII protein coat is consistent with the possibility that



extended and large cargo is transported in tubular sections (as depicted schematically in Fig. 3g) or in ‘super-sized’ COPII bulges.

In vitro, vesicle strings developed to remarkable dimensions of dozens of connected vesicles, several micrometers in total length (Fig. 2b–d), which supports the notion of Bannykh et al.¹⁵ that vesicle separation fails in the absence of GTP hydrolysis. To exclude extraneous effects of non-hydrolysable GTP analogs, we used hydrolysable GTP and replaced wtSar1p by Sar1p(H77L) (Fig. 2j). The intrinsic GTPase activity of this mutant is similarly low as that of wtSar1p, but stimulation of the GTPase activity by the Sec23/24p complex is reduced from about 9-fold to 2-fold³. The lowered GTPase activity of the mutant in the presence of the full COPII complex proved sufficient for the formation of rigid, multibudded extensions (Fig. 2j, Movie S3, Fig. 3k), as seen with the non-hydrolysable GTP analog.

Our *in vitro* data illustrates that a block of GTP hydrolysis generates unfissioned precursors of COPII vesicles. This result leaves the question open how GTP hydrolysis and fission are controlled. Incubations containing GTP instead of GMP-PNP on artificial giant liposomes did not generate separate vesicles on an appreciable scale. The less dramatic GUV morphology change observed with COPII/GTP (Fig. 2h,i) is consistent with the finding that, with GTP, lipid bilayers fail to retain the membrane-bound COPII coat as measured in light scattering experiments¹⁷ and during density gradient sedimentation¹. Coat stability was enhanced by the nucleotide exchange factor Sec12ΔCp compared to the less active nucleotide exchange facilitated by lowering Mg²⁺ with EDTA¹. Presumably, Sec12ΔCp allows multiple rounds of nucleotide hydrolysis and exchange. In agreement, COPII/GTP reactions had a stronger morphological effect on GUVs in the presence of Sec12ΔCp than with EDTA (Fig. 2h vs. 2i), whereas no difference between EDTA and Sec12ΔCp was observed in incubations containing GMP-PNP (Fig. 2c vs. 2b).

Obviously, uninhibited large-scale disintegration of a lipid bilayer into vesicles is not desirable in cells. A complex interplay of factors may be necessary to regulate vesicle fission processes, as suggested in a study of COPI assembly on GUVs, where membranes also failed to undergo fission¹⁸. Regulation of COPII vesicle fission *in vivo* may be provided through the localization of specific factors (Sec16p and membrane-anchored Sec12p, for instance) and by triggering events, such as the sorting of cargo proteins into buds, as suggested by Tabata et al.¹⁹. The regulation of Sar1p-mediated GTP hydrolysis in relation to membrane fission requires further investigation.

One hypothesis for a fission pathway⁹ postulates that GTP hydrolysis leads to unbinding of the Sar1 amphipathic helix from the membrane, resulting in packing defects. Such defects should lead to rapid changes in membrane morphology to fill the gaps and avert the energetically unfavorable exposure of the hydrophobic lipid chains to water. To preclude simple contraction (i.e., shortening of the lipid tubule) as a path of relaxation, a separation force may be needed. Separation forces can be static, i.e. maintaining the length of the protrusion, or dynamic, i.e. actively extending the protrusion. Static separation forces, applied artificially by attachments to an EM grid, have been reported to support fission of dynamin-mediated tubular constrictions^{20,21}. *In vivo*, dynamic separation forces may be exerted by motor proteins and cytoskeleton, for example, by dynactin/dynein coupling to Sec23p²². Here, we observed that tubules formed by COPII were, despite their constrictions, globally rigid over several micrometer (Fig. 3b, Movie S2), demonstrating that the COPII scaffold conveys rigidity and directionality including at the necks between the bulges. The coat may thus itself act as an ‘exoskeleton’, providing a static separation force between the bulges and obviating the need for cytoskeleton involvement in simple COPII budding.

Furthermore, coat completion may actively contribute to fission. In the absence of Sar1p and membranes, the coat has a propensity to

assemble into spherical structures, which have positive curvature in both principal directions^{12,23}. This propensity may help to promote the transition from tubular membranes, which have positive curvature in only one direction, to vesicles, which have positive curvature in both directions (Fig. 3c).

Methods

Giant Unilamellar Vesicles. GUVs were produced by a modification of the electroformation method²⁴. The ‘Major-Minor mix’ of lipids⁸ was prepared, consisting of the phospholipids DOPC (1,2-dioleoyl-sn-glycero-3-phosphocholine, 51 mol%), DOPE (1,2-dioleoyl-sn-glycero-3-phosphoethanolamine, 22 mol%), DOPS (1,2-dioleoyl-sn-glycero-3-[phospho-L-serine], 8 mol%), DOPA (1,2-dioleoyl-sn-glycero-3-phosphate, 5 mol%), soy PI (L-α-phosphatidylinositol, 8 mol%), porcine brain PI4P (L-α-phosphatidylinositol-4-phosphate, 2.2 mol%), porcine brain PI(4,5)P2 (L-α-phosphatidylinositol-4,5-bisphosphate, 0.8 mol%), CDP-DAG (1,2-dioleoyl-sn-glycero-3-(cytidine diphosphate), 2 mol%); all lipids from Avanti Polar Lipids, Alabaster, AL), fluorescent lipid analog (1 mol%, see below) and ergosterol (Sigma, St. Louis, MO; 20% ergosterol by weight, 80% phospholipids by weight). As fluorescent lipid analogs, DiIC18 (1,1'-dioctadecyl-3,3,3',3'-tetramethylindocarbocyanine perchlorate, Invitrogen, Carlsbad, CA; for single-color confocal microscopy), DiDC18 (1,1'-dioctadecyl-3,3,3',3'-tetramethylindocarbocyanine perchlorate, Invitrogen; for two-color confocal microscopy) and Texas-Red DHPE (Texas Red-1,2-dihexadecanoyl-sn-glycero-3-phosphoethanolamine, Invitrogen) were used.

Lipids were combined in chloroform:methanol (2:1, volume ratio) at 10 mg/ml total concentration and dried as a thin layer on indium-tin-oxide coated glass slides (Delta Technologies, Stillwater, MN). The slides were assembled to form a chamber by using 3 mm thick silicon spacers and holding the slides together with office clips. The chamber was filled with sucrose solution (540 mOsmol/kg) and electroformation was performed overnight using an approximately 3 Volt, 10 Hz sinusoidal voltage and copper conductive tape (3M, SPI supplies) for connections. The GUVs were harvested by sedimentation in an iso-osmolar glucose solution at 4°C.

COPII proteins. Yeast COPII proteins were expressed and purified as previously described^{2,25–29}. The H77L mutation was introduced into Sar1p by site-directed mutagenesis with Pfu polymerase (Stratagene) using the coding sequence of Sar1p in the vector pTY40²⁸. Correct DNA sequences were confirmed by sequencing. Green fluorescent Sec13/31 protein was produced by reacting purified Sec13/31p with a 20-fold excess of Alexa 488 maleimide (Invitrogen), followed by purification on a size exclusion column. Alexa 488 labeled Sec13/31p was mixed at 40:60 molar ratio with unlabeled Sec13/31p.

***In vitro* reconstitution.** The purified proteins were mixed at the indicated final concentrations with HKM buffer (20 mM HEPES, pH 6.8, 160 mM potassium acetate, 1 mM magnesium chloride, final concentrations). Nucleotide exchange was accelerated either by chelating Mg²⁺ with 2.5 mM EDTA (Fig. 2b,d,e, 3a–h_j), or by the addition of Sec12ΔCp (Fig. 2c,f,g,j, 3k). Glycerol was used at variable concentrations to obtain a final osmolarity of approx. 600 mOsmol/kg. Concentrated GUVs were added to the osmolarity-adjusted protein solutions at 1:20 (vol:vol) dilution. Incubations of GUVs with COPII proteins were performed at room temperature (≈23°C).

Microscopy. Confocal microscopy was performed on a Zeiss LIVE upright microscope and on a Zeiss LSM 710 inverted microscope (Carl Zeiss Microimaging, Jena, Germany), using 40× water immersion C-Apochromat objectives, with an NA of 1.1 and 1.2, respectively. Imaging chambers consisted of coverslips coated with gelatin (Sigma), which were held together and sealed by double-sided tape.

For cryo-EM, samples were incubated directly on holey carbon grids (Fig. 3d,e,h) or incubated in a tube and pipetted onto a grid (Fig. 3a,b,f,g). Samples were vitrified by plunge freezing the grid. Imaging was performed on a Tecnai F30 electron microscope (FEI, Eindhoven, Netherlands), equipped with a 4K FEI Eagle camera. The microscope was operated at 300 kV, with a magnification of 20,000×, giving a pixel size of 0.59 nm at the specimen level. Data was collected at −4 μm defocus with an electron dose of 15–25 e[−] Å^{−2}. The lighter areas in Fig. 3a,d–h represent the 2 μm diameter holes in the carbon support.

For negative staining, samples were incubated in a tube and spread onto a nickel grid coated with Formvar (Plano, Wetzlar, Germany). Excess liquid was blotted off with filter paper, the grid was stained with 1% aqueous uranyl acetate and excess staining solution was blotted off. Dried specimens were examined on a Zeiss EM 900 transmission electron microscope.

The thin section electron microscopy image of a fibroblast cell (Fig. 3i) was obtained as described¹⁴ and kindly provided by Lelio Orci (Faculty of Medicine, University of Geneva).

1. Futai, E., Hamamoto, S., Orci, L. & Schekman, R. GTP/GDP exchange by Sec12p enables COPII vesicle bud formation on synthetic liposomes. *EMBO J.* **23**, 4146–4155 (2004).
2. Lee, M. C. et al. Sar1p N-terminal helix initiates membrane curvature and completes the fission of a COPII vesicle. *Cell* **122**, 605–617 (2005).



3. Saito, Y., Kimura, K., Oka, T. & Nakano, A. Activities of mutant Sar1 proteins in guanine nucleotide binding, GTP hydrolysis, and cell-free transport from the endoplasmic reticulum to the Golgi apparatus. *J. Biochem.* **124**, 816–823 (1998).
4. Aridor, M., Bannykh, S. I., Rowe, T. & Balch, W. E. Sequential coupling between COPII and COPI vesicle coats in endoplasmic reticulum to Golgi transport. *J. Cell Biol.* **131**, 875–893 (1995).
5. Bielli, A. *et al.* Regulation of Sar1 NH2 terminus by GTP binding and hydrolysis promotes membrane deformation to control COPII vesicle fission. *J. Cell Biol.* **171**, 919–924 (2005).
6. Long, K. R. *et al.* Sar1 assembly regulates membrane constriction and ER export. *J. Cell Biol.* **190**, 115–128 (2010).
7. Tsafir, I. *et al.* Pearling instabilities of membrane tubes with anchored polymers. *Phys. Rev. Lett.* **86**, 1138–1141 (2001).
8. Matsuoka, K. *et al.* COPII-coated vesicle formation reconstituted with purified coat proteins and chemically defined liposomes. *Cell* **93**, 263–275 (1998).
9. Antony, B. Membrane deformation by protein coats. *Curr. Opin. Cell Biol.* **18**, 386–394 (2006).
10. Pucadyil, T. J. & Schmid, S. L. Conserved functions of membrane active GTPases in coated vesicle formation. *Science* **325**, 1217–1220 (2009).
11. Kuehn, M. J., Herrmann, J. M. & Schekman, R. COPII-cargo interactions direct protein sorting into ER-derived transport vesicles. *Nature* **391**, 187–190 (1998).
12. Stagg, S. M. *et al.* Structural basis for cargo regulation of COPII coat assembly. *Cell* **134**, 474–484 (2008).
13. O'Donnell, J., Maddox, K. & Stagg, S. The structure of a COPII tubule. *J. Struct. Biol.* **173**, 358–364 (2011).
14. Fromme, J. C. *et al.* The genetic basis of a craniofacial disease provides insight into COPII coat assembly. *Dev. Cell* **13**, 623–634 (2007).
15. Bannykh, S. I., Rowe, T. & Balch, W. E. The organization of endoplasmic reticulum export complexes. *J. Cell Biol.* **135**, 19–35 (1996).
16. Zeuschner, D. *et al.* Immuno-electron tomography of ER exit sites reveals the existence of free COPII-coated transport carriers. *Nat. Cell Biol.* **8**, 377–383 (2006).
17. Antony, B., Madden, D., Hamamoto, S., Orci, L. & Schekman, R. Dynamics of the COPII coat with GTP and stable analogues. *Nat. Cell Biol.* **3**, 531–537 (2001).
18. Manneville, J. B. *et al.* COPI coat assembly occurs on liquid-disordered domains and the associated membrane deformations are limited by membrane tension. *Proc. Natl. Acad. Sci. U. S. A.* **105**, 16946–16951 (2008).
19. Tabata, K. V. *et al.* Visualization of cargo concentration by COPII minimal machinery in a planar lipid membrane. *EMBO J.* **28**, 3279–3289 (2009).
20. Danino, D., Moon, K. H. & Hinshaw, J. E. Rapid constriction of lipid bilayers by the mechanochemical enzyme dynamin. *J. Struct. Biol.* **147**, 259–267 (2004).
21. Lenz, M., Morlot, S. & Roux, A. Mechanical requirements for membrane fission: common facts from various examples. *FEBS Lett.* **583**, 3839–3846 (2009).
22. Watson, P., Forster, R., Palmer, K. J., Pepperkok, R. & Stephens, D. J. Coupling of ER exit to microtubules through direct interaction of COPII with dynactin. *Nat. Cell Biol.* **7**, 48–55 (2005).
23. Fath, S., Mancias, J. D., Bi, X. & Goldberg, J. Structure and organization of coat proteins in the COPII cage. *Cell* **129**, 1325–1336 (2007).
24. Angelova, M. I. & Dimitrov, D. S. Liposome Electroformation. *Faraday Discuss. Chem. Soc.* **81**, 303–311 (1986).
25. Shimoni, Y. & Schekman, R. Vesicle budding from endoplasmic reticulum. *Methods Enzymol.* **351**, 258–278 (2002).
26. Futai, E. & Schekman, R. Purification and functional properties of yeast Sec12 GEF. *Methods Enzymol.* **404**, 74–82 (2005).
27. Bi, X., Corpina, R. A. & Goldberg, J. Structure of the Sec23/24-Sar1 pre-budding complex of the COPII vesicle coat. *Nature* **419**, 271–277 (2002).
28. Barlowe, C. *et al.* COPII: a membrane coat formed by Sec proteins that drive vesicle budding from the endoplasmic reticulum. *Cell* **77**, 895–907 (1994).
29. Salama, N. R., Chuang, J. S. & Schekman, R. W. Sec31 encodes an essential component of the COPII coat required for transport vesicle budding from the endoplasmic reticulum. *Mol. Biol. Cell* **8**, 205–217 (1997).

Acknowledgements

We thank Bob Lesch and Crystal Chan for help with protein purifications, James Riches for help with cryo-EM, Holly Aaron (MIC, Berkeley) for assistance with confocal and Gerd Hause (Halle) with electron microscopy. We thank Lelio Orci (Faculty of Medicine, University of Geneva) for providing Fig. 3I. We are grateful to current and former members of the labs of Randy Schekman, Jay Groves, George Oster and David Drubin for help and discussions, especially Chao-Wen Wang, Raghuvveer Parthasarathy, John Tran, and Bruno Antony. K.B. acknowledges a postdoctoral fellowship of the Deutsche Akademie der Naturforscher Leopoldina (BMBF-LPD-9901/8-160). K.B., A.M., S.D. and D.G. were supported by the BMBF ZIK program (FKZ 03Z2HN22) and ERDF grant 1241 09 0001. R.S. and K.B. were supported by the Howard Hughes Medical Institute.

Author contributions

K.B., J.A.G.B. and R.S. designed the project, K.B., E.F., S.P., A.M., S.D., D.G. carried out experiments, K.B., J.A.G.B., R.S. evaluated data, K.B. and R.S. wrote the paper.

Additional information

Supplementary Information accompanies this paper at <http://www.nature.com/scientificreports>

Competing financial interests: The authors declare no competing financial interests.

License: This work is licensed under a Creative Commons Attribution-NonCommercial-ShareAlike 3.0 Unported License. To view a copy of this license, visit <http://creativecommons.org/licenses/by-nc-sa/3.0/>

How to cite this article: Bacia, K. *et al.* Multibudded tubules formed by COPII on artificial liposomes. *Sci. Rep.* **1**, 17; DOI:10.1038/srep00017 (2011).